جامعة الملك عبدالله
للعلوم والتقنية
King Abdullah University of
Science and Technology

Decadal Stability of Red Sea Mangroves

Item Type	Article
Authors	Almahasheer, Hanan; Aljowair, Abdulaziz; Duarte, Carlos M.; Irigoien, Xabier
Citation	Decadal Stability of Red Sea Mangroves 2015 Estuarine, Coastal and Shelf Science
Eprint version	Post-print
DOI	10.1016/j.ecss.2015.11.027
Publisher	Elsevier BV
Journal	Estuarine, Coastal and Shelf Science
Rights	NOTICE: this is the author's version of a work that was accepted for publication in Estuarine, Coastal and Shelf Science. Changes resulting from the publishing process, such as peer review, editing, corrections, structural formatting, and other quality control mechanisms may not be reflected in this document. Changes may have been made to this work since it was submitted for publication. A definitive version was subsequently published in Estuarine, Coastal and Shelf Science, 15 December 2015. DOI: 10.1016/j.ecss.2015.11.027
Download date	04/08/2022 16:45:01
Link to Item	http://hdl.handle.net/10754/584005

Accepted Manuscript

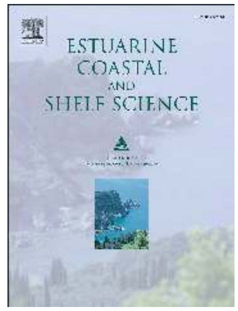

Decadal Stability of Red Sea Mangroves

Hanan Almahasheer, Abdulaziz Aljowair, Carlos M. Duarte, Xabier Irigoien

PII: S0272-7714(15)30149-9

DOI: 10.1016/j.ecss.2015.11.027

Reference: YECSS 4966

To appear in: *Estuarine, Coastal and Shelf Science*

Received Date: 14 June 2015

Revised Date: 16 November 2015

Accepted Date: 28 November 2015

Please cite this article as: Almahasheer, H., Aljowair, A., Duarte, C.M., Irigoien, X., Decadal Stability of Red Sea Mangroves, *Estuarine, Coastal and Shelf Science* (2016), doi: 10.1016/j.ecss.2015.11.027.

This is a PDF file of an unedited manuscript that has been accepted for publication. As a service to our customers we are providing this early version of the manuscript. The manuscript will undergo copyediting, typesetting, and review of the resulting proof before it is published in its final form. Please note that during the production process errors may be discovered which could affect the content, and all legal disclaimers that apply to the journal pertain.

ACCEPTED MANUSCRIPT

Decadal Stability of Red Sea Mangroves

Hanan Almahasheer[1,2,*], Abdulaziz Aljowair [3], Carlos M. Duarte[1] and Xabier Irigoien[1]

[1] King Abdullah University of Science and Technology (KAUST), Red Sea Research Center, Thuwal 23955-6900, Kingdom of Saudi Arabia

[2] Biology Department, University of Dammam (UOD), Dammam 31441-1982, Kingdom of Saudi Arabia

[3] Space Research Institute, King Abdul Aziz City for Science and Technology (KACST), Riyadh 11442-6086, Kingdom of Saudi Arabia

*: Corresponding author: Xabier.Irigoyen@kaust.edu.sa

ACCEPTED MANUSCRIPT

ACCEPTED MANUSCRIPT

Abstract

Across the Earth, mangroves play an important role in coastal protection, both as nurseries and carbon sinks. However, due to various human and environmental impacts, the coverage of mangroves is declining on a global scale. The Red Sea is in the northern-most area of the distribution range of mangroves. Little is known about the surface covered by mangroves at this northern limit or about the changes experienced by Red Sea mangroves. We sought to study changes in the coverage of Red Sea mangroves by using multi-temporal Landsat data (1972, 2000 and 2013). Interestingly, our results show that there has been no decline in mangrove stands in the Red Sea but rather a slight increase. The area covered by mangroves is about 69 Km^2 along the African shore and 51 Km^2 along the Arabian Peninsula shore. From 1972 to 2013, the area covered by mangroves increased by about 0.29% y^{-1}. We conclude that the trend exhibited by Red Sea mangroves departs from the general global decline of mangroves. Along the Red Sea, mangroves expanded by 12% over the 41 years from 1972 to 2013. Losses to Red Sea mangroves, mostly due to coastal development, have been compensated by afforestation projects.

Keywords: Remote sensing, GIS, Mapping, Satellite, Landsat, NDVI and Distribution.

1. Introduction

Mangroves form highly productive ecosystems, providing habitat for marine and terrestrial species (Nagelkerken et al., 2008), protecting coastal areas from storms and sea level rises (Koch et al., 2009), and acting as intense carbon sinks (Donato et al., 2011). Unfortunately, mangroves are found within the most threatened ecosystems on Earth; about 1/3 of their global area has been lost since World War II (Alongi, 2002). This decline continues at an annual rate of about 2.1% (Valiela et al., 2001). A recent assessment of regional mangrove trends, however, showed that reported rates were highly variable between regions (Friess and Webb, 2014). These reports identify aquaculture and urban developments as the main drivers of mangrove decline across these regions (FAO, 2007).

The Red Sea is adjacent to the northern limit of the Indo-Pacific mangrove, located in the Sinai Peninsula at 28°N. Along the Red Sea, mangroves experience some of the most difficult conditions in their distribution range, including no permanent freshwater inputs, salinities over 40 ppt, sea surface temperatures over 31 ^{o}C in summer and recent abrupt warming of the sea (Raitsos et al., 2011). On the other hand, urban development and aquaculture in the Red Sea are comparatively limited and, because the desert nature of the coast, direct anthropogenic impacts have been relatively contained. The Red Sea therefore provides a good model to study the resilience of mangrove ecosystems to harsh environmental conditions with as yet limited direct anthropogenic impacts. Even so, information on the area covered by Red Sea mangroves and on changes in this area over time is scarce and often reported only in grey literature at national levels. The world atlas of mangroves (Spalding et al., 2010) reports that Red Sea mangroves are scattered along the coast of Djibouti, cover only 500 ha in Egypt, while in Sudan they are found around creeks and near-shore islets. Eritrea's mangroves are patchy and distributed along approximately 380 km of shoreline (De Grissac and Negussie, 2007), while mangroves are abundant along Yemen's Red Sea coast although mostly absent along the Gulf of Aden coastline in Yemen (Spalding et al., 2010). Mangroves are found as fragmented stands in the intertidal zones of the Red Sea coast of Saudi Arabia (Kumar et al., 2010). An additional study (El-Juhany, 2009) reported that mangrove stands covered an area of 36.15 Km^2 between the southern border of Saudi Arabia in Jazan to the Jeddah's southern corniche. One-third (35%) of this area was in Jazan (12.77 Km^2), while the remaining two-thirds (65%) was in Makkah and Asir (23.38 Km^2) Provinces.

Although FAO (FAO, 2007) described the status of mangroves in the Red Sea from 1980-2005, a comprehensive assessment of the area covered by mangroves and of the stability of this area along the Red Sea is still lacking. Assessments of the areas occupied by mangroves and of any changes to these areas are fundamental to the estimation of the ecological services provided by the mangroves in the region. In addition, such assessments inform conservation plans and provide basic information to improve our understanding of the resilience of mangrove ecosystems to harsh environmental conditions and warming. Here, we report changes in the status and distribution of Red Sea mangroves over 41 years, from 1972 to 2013, using Landsat images to determine the area and stand structure of mangroves in the Red Sea and their dynamics over the past four decades.

2. Methods

Satellite imagery

ACCEPTED MANUSCRIPT

We used Erdas Imagine V9.3 and ArcGIS 10.2 to assess mangrove vegetation along the Arabian Peninsula and African coastlines of the Red Sea based on the analysis of Landsat images for three periods: 1972, when the first satellite in the series (Landsat 1) was launched (Chander et al., 2009) to 2013 (Landsat 8), and including 2000 (Landsat 7). Briefly, the Landsat 1 mission carried a Multispectral Scanner (MSS) sensor with a resolution of 60 m, whereas the sensors on board the Landsat 7 and 8 missions were Enhanced Thematic Mapper (ETM) and Enhanced Thematic Mapper plus (ETM+), respectively, both with resolutions of 30 m (Chander et al., 2009). The Landsat 8 mission also carried an Operational Land Imager (OLI) and a Thermal Infrared Sensor (TIRS), with resolution of 30 m (Lulla et al., 2013). Details on the images used in the study are provided in the supplementary materials (Tables S1, S2, and S3). The data set is available in PANGAEA (http://www.pangaea.de).[1]

Data processing

Vectors were drawn to delineate the coastline because mangroves in the Red Sea only occur along the coastline because there are no permanent rivers and estuaries. Furthermore, the desert reaches to the coast around the Red Sea and large vegetation along the coastline is limited to mangroves. This means that classification problems are limited to presence/absence of vegetation. We applied an atmospheric correction to the data in which the pixels were converted to top of atmosphere (TOA) spectral radiances using the radiance rescaling factors provided in the metadata file: $L_\lambda = M_L Q_{cal} + A_L$ (USGS_Landsat_Missions, 2013), except for the 1972 images, which were corrected by the

[1] The data set will be published at the time of acceptance of the paper.

local data provider. The Normalized Difference Vegetation Index (NVDI) was used to estimate the vegetation in the coastal fringe, through unsupervised classification. Briefly, NVDI uses near-infrared and red light reflected by the vegetation and captured by the sensor of the satellite to measure absorbance of red light by chlorophyll and the reflection of near-infrared by the mesophyll leaf structure (Pettorelli et al., 2005). NDVI values range from -1 to +1, where any value below zero does not correspond to green vegetation (Hunink et al., 2010). Hence, the images were classified using the NDVI >0 as mangrove and NDVI ≤ 0 as non-mangrove. The robustness of this classification was verified through the ground referencing (see below). This index was applied only to the areas where mangroves were expected to occur (i.e., vegetation along the coastline and coastal vegetation on islands). Inland and open-sea areas were excluded because mangroves do not occur in such areas (Giri et al., 2011). We generated vegetation thematic images and shape files assuming that that any green vegetation farther than 1 kilometer from the coast was not mangrove. Images were mosaicked and the surface of the mangroves was estimated using ArcGIS from the shape files and retrieving the area for each mangrove stand located along the Red Sea coast. Mapcarta and British Admiralty Maps (numbers 158,171, 10,116, and 1157) were used as sources for the location names. Moreover, we used four high-resolution images (GeoEye Satellite) of the central Red Sea and Google maps to verify that no other type of vegetation besides mangroves can be found along the Red Sea coast.

Accuracy assessment

The assessment of mangrove vegetation was crosschecked with ground-referencing data in various ways: using reported locations where mangroves occurred in 1972 and

2000 (Price et al., 1987), visiting a number of locations along a 90 Km strip of coastline between Thuwal and Khor Alkharar between December 2014 and March 2015, and using Google Earth products to verify the classification of mangrove stands in remote locations.

To estimate the accuracy of our estimates, we applied a 100-meter buffer around the coast, then randomly selected 500 points to be crosschecked with the vegetation shape files for 2013. Out of the 500 points, 158 were positive for vegetation in the shape files and 342 were negative. Then we visually checked each of the 500 points on Google Earth to determine that 16 out of the 158 were not mangroves (i.e. false positives) and 26 out of the 342 classified as non-mangrove did have mangroves (false negatives). These results were used to calculate the accuracy of the classification (Congalton and Green, 2008; Fatoyinbo and Simard, 2013), resulting in an accuracy of 91.6% (Table 1, Fig. S4).

Error estimates

We also assessed the error associated with our estimates of stand size by analyzing two to three replicate images along with the original image for different locations in each of the study periods (Supplementary material, Table S5). The resulting estimate of uncertainty around the areas covered by mangrove stands was then propagated, by drawing, for each stand, replicated area estimates randomly from a normal distribution with the mean equal to the estimated area and the standard deviation calculated from the estimated coefficient of variation of area estimates for each year, was calculated from the average and standard deviation and reported as a percentage. (Supplementary material, Tables S1, S2, S3, S5 and S6). This error propagation allowed us to calculate a standard error for the estimates of the total area covered by Red Sea mangroves in each year and was used to assess the significance of changes to the total area over time.

We examined the frequency distribution of mangrove stands along the Red Sea using a Pareto distribution (Vidondo et al., 1997), after removing all stands smaller than 0.00026 Km^2 in size to account for the difference in pixel size between the 1972 and subsequent images used in this study.

3. Results

Ground-referencing data

Ground referencing data confirmed the reliability of the classification of the presence or absence of mangroves (with an overall accuracy of 91.6%, Table 1, Fig. S4). The coefficient of variation in the assessment of the area covered by individual mangrove stands ranged from 23 to 35.9 % (Table S6), which is substantial due to the small size of individual patches (median patch area of Red Sea mangroves 0.00721, 0.00878 and 0.00948 Km^2 for 1972, 2000 and 2013, respectively, Table S7). Our error estimates were relatively high due to the small size of individual mangrove stands along the Red Sea, which made them conducive to edge effects. In addition, uncertainty derived from the interference of high tides in detecting the mangroves increased the error estimates.

Estimating mangrove cover

The mapped Red Sea mangroves included stands located all along the African and Arabian Peninsula coasts of the Red Sea, extending all the way to the strait of Bab-el-Mandeb where the Red Sea opens to the Indian Ocean (Fig. 1a)(28.20893°N to 27.67161°N in 1972, 28.207348°N to 27.671217°N in 2000 and 28.207302°N to 27.671293°N in 2013). The images showed that the abundance of mangroves increase from north to south along the Red Sea (Figs. 1a, b and Table S8).

The estimated total area of Red Sea mangroves increased significantly (Tukey HSD posthoc test, $P < 0.05$) from 120 ± 0.54 Km^2 in 1972 to 132 ± 0.94 Km^2 in 2000, and no significant change, within the power of our analysis, was detected between 2000 and 2013 (Tukey HSD posthoc test, $P > 0.05$) when the area was estimated at 135 ± 0.86 Km^2 (Fig. 2). The increase between 1972 and 2000 was mainly due to an increase in mangrove stands along the African shore, where the area of mangroves increased from 69 Km^2 to 77 Km^2, compared with a change from 51 Km^2 to 55 Km^2 along the Arabian Peninsula (Figs.1band 2).

We identified about 5,000 mangrove patches along the Red Sea (2234 in 1972, 5765 in 2000 and 5157 in 2013). These patches had linear dimensions greater than 60 m in 1972 and greater than 30 m in 2000 and 2013, the pixel size of the Landsat images used. The much greater number of patches in 2000 and 2013 compared with in 1972 indicates both the appearance of new patches and the detection of smaller patches not identified in the 1972 images. Indeed, the number of patches detectable with the Landsat 1 resolution would be 2233 in 1972, then 2381 and 2234, 2000 and 2013, respectively. The increased resolution in 2000 and 2013 had, however, only a small effect on the area estimates, as shown by the mangrove areas that were estimated when patches too small to be detected in 1972 images were excluded (128.7 Km^2 in 2000 and 131.8 Km^2 in 2013). They contributed only 2.7 % and 2.0 % of the total mangrove area detected in 2000 and 2013, respectively (total area 132.4 Km^2 in 2000 and 135.1 Km^2 in 2013). Hence, the increase in mangrove area between 1972 and 2000 (Fig. 3) remains significant even after accounting for the increased resolution in 2000 and 2013. Future efforts at mapping mangroves in the Red Sea should use high-resolution satellites, such as GeoEye with 0.5 m resolution, to resolve smaller patches than those we could resolve here is recommended to be used if the temporal changes are not needed for the study.

The size distribution of Red Sea mangrove patches was highly skewed and conformed to a Pareto distribution with a cut-off represented by steeper decline than expected for a Pareto distribution for patches larger than 0.4 Km^2, which comprised less than 3 % of all patches (Fig. 3). Most of the mangrove stands were composed of small mangrove patches, with only 10% of the patches larger than 0.096 Km^2 and only 1% of them larger than 0.87 Km^2 (Fig. 3). When patches smaller than 0.00026 Km^2, too small to be detected in the 1972 images, were excluded to avoid biasing the comparison, the median size as well as the 90% and 99% percentiles of the patches tended to increase significantly (Student's t-test , $P<0.05$) over time (Fig. 3, Supplementary material, Table S7).

Losses and gains over time

Examination of the balance between losses and gains showed that there was a prevalence of increases, particularly along the African shore (Table 2, Fig 4). The largest mangrove stand along the Red Sea, located along the Alwajh Bank (Tabuk, Saudi Arabia), remained in an approximately steady state over the 41 years of study (1972 = 3.8 Km^2, 2000 = 4.5 Km^2, 2013 = 4.3 Km^2, Fig. 5A). A successful rehabilitation project in Yanbu, Saudi Arabia, resulted in a 50-fold increase in the area covered by mangroves (1972 = 0.011 Km^2, 2000 = 0.543 Km^2, 2013 = 0.562 Km^2) in this region (Fig. 5B). In contrast, a decline was detected in a costal lagoon in Alith, Saudi Arabia, where one of the largest shrimp farms in the world was established in 1986. Mangrove stands in the lagoon occupied 2.33 km^2 in 1972 and declined to 1.91 Km^2 in 2000 and 0.18 Km^2 in 2013 (Fig. 5C). Thorough documentation of potential drivers of losses and gains is presented in Supplementary material, Table 9, with an illustration of these drivers in Fig. 6.

4. Discussion

Red Sea mangrove forests are dominated by small patches, with a median size of only 0.007 to 0.009 Km^2. The fact that the median patch size was similar between years despite a major increase in resolution of the images between 1972 and 2013 indicates that the estimate is robust and independent of the change in resolution of the images. Although the area covered is relatively modest, mangroves are the most important vegetated habitats in the region, which is characterized by inland deserts along both the African and Arabian Peninsula shores.

The largest mangrove stand in the Red Sea occurs along the Alwajh Bank (Tabuk, Saudi Arabia) where extensive mangrove and seagrass beds can be found (Bruckner, 2011). Along the African shore, the largest stands are found along the coast of Eritrea. We found mangrove stands to be patchy in the northern Red Sea and to increase, in area and patch size, to the south, as reported in the past (Mandura, 1997). A range of factors may explain this pattern, including higher minimum air temperatures, lower salinity, higher rainfall and freshwater supply and increased nutrient concentrations towards the south (Saifullah, 1996). Also, a shift in sediment composition from stony corals in the north to fine sediment in the south would favor mangrove growth (Price et al., 1987).

Mangrove forests are experiencing a decline around the world due to logging, land reclamation and conversion of mangrove forests into aquaculture farms (Polidoro et al., 2010), causes connected with the growth rate of the human population with 60% of the population living in coastal regions (Green et al., 1996). Although Red Sea nations are also experiencing population growth 1.8 to 5.1 % per annum (PERSGA, 2002), our analysis did not provide evidence of major losses of mangrove stands over the past four decades. On the contrary, the areas covered by Red Sea mangrove stands increased significantly, by 15 Km^2 (11 Km^2 when excluding the patches too small to have been detected in 1972), or 12 %, during the study period. This expansion is supported by a tendency for the size of individual stands to expand between 1972 and 2000. Two-thirds of the area gained by mangroves is located along the African shore, particularly along Eritrea, where large mangrove stands are located. The recent expansion of mangroves along the Red Sea coast of Saudi Arabia is in contrast to the major loss of mangroves along the Arabian Gulf Coast of Saudi Arabia, where over 55 % of the area of mangroves was lost from 1972 to 2011 (Almahasheer et al., 2013).

The expansion of mangroves between 1972 and 2000 is the net result of the balance between losses and gains. Whereas a significant expansion of mangrove area was observed between 1972 and 2000, losses and gains between 2000 and 2013 compensated each other within the uncertainty of our analysis, so no significant change in total mangrove area in the Red Sea was detected in the later period. Afforestation projects contributed to gains in several areas, including those in Yanbu, Saudi Arabia, and the Manzanar mangrove restoration project conducted in the mid 1990's in Hirgigo, Eritrea (De Grissac and Negussie, 2007). Losses were mostly due to coastal development and pollution, particularly

ACCEPTED MANUSCRIPT

along the Saudi coast, whereas along the coasts of Yemen and Africa, losses were due to overgrazing by camels and logging (Table S9). Whereas camel grazing would degrade mangroves, but generally not lead to losses, events of intense degradation have been reported, such as the heavy impact of camel grazing on 500 ha of mangrove around Port of Sudan by camel grazing (Bojang, 2009). Moreover, camel grazing, which is likely to be a pressure of mangroves intrinsic to the Red Sea, may prevent gains by removing seedling recruits. Compensatory afforestation projects associated with some projects, such as the construction of the King Abdullah University of Science and Technology in Thuwal, Saudi Arabia, proved effective in compensating for the losses during the development phase. One of the mangrove stands experiencing losses was that located in Alith, Saudi Arabia, where a large aquaculture farm was built in the late 1980's. However, the decline cannot be directly related to the construction of the aquaculture facilities, as suggested by (Gladstone et al., 1999), because the mangrove ponds were excavated inland and the decline of mangroves at Alith occurred between 2000 and 2013, 10 years after the construction and the start of operations of the aquaculture farm. Similarly, 58% of African mangroves were destroyed before shrimp aquaculture developed in the region (Sadek et al., 2002).

In summary, the results presented here show that Red Sea mangroves depart from the general declining trend of mangroves elsewhere, exhibiting an expansion, by 12% in area, over 41 years from 1972 to 2013. This expansion is the net result of the balance between losses and gain, where afforestation projects have played an important role in maintaining, and expanding mangroves along the Red Sea. However, coastal development in the region, including major infrastructure projects for ports and tourism, may represent a threat in the future unless mangrove conservation receives prominent attention as a required milestone at the planning stage.

6. Acknowledgement

We thank the Space Research Institute in King Abdul-Aziz city for Science and Technology (KACST) for providing the raw data. We also thank Virginia Unkefer for reviewing the manuscript and M. Campbell for help with accuracy assessment. This research was supported by the baseline funding provided by King Abdullah University of Science and Technology to Xabier Irigoien.

7. References:

Almahasheer, H., Al-Taisan, W., Mohamed, M.K., 2013. Mangrove Deterioration in Tarut Bay on the Eastern Province of the Kingdom of Saudi Arabia. Pakhtunkhwa J. Life Sci 01, 49-59.
Alongi, D.M., 2002. Present state and future of the world's mangrove forests. Environmental conservation 29, 331-349.
Bojang, E., 2009. The relevance of mangrove forests to African fisheries, wildlife and water resources. Food And Agriculture Organisation of the United Nations. Accra, Ghana.
Bruckner, A., 2011. Khaled bin Sultan Living Oceans Foundation Habitat Mapping and Characterization of Coral Reefs of the SaudiArabian Red Sea: 2006-2009. Panoramic Press, Arizona, 140 pp.
Chander, G., Markham, B.L., Helder, D.L., 2009. Summary of current radiometric calibration coefficients for Landsat MSS, TM, ETM+, and EO-1 ALI sensors. Remote sensing of environment 113, 893-903.
Congalton, R.G., Green, K., 2008. Assessing the accuracy of remotely sensed data: principles and practices. CRC press.
De Grissac, A., Negussie, K., 2007. State of the Coast Eritrea, 2006-2007. Eritrea‟ s Coastal Marine and Island Biodiversity Conservation Project, UNDP-Eritrea, 22.
Donato, D.C., Kauffman, J.B., Murdiyarso, D., Kurnianto, S., Stidham, M., Kanninen, M., 2011. Mangroves among the most carbon-rich forests in the tropics. Nature Geoscience 4, 293-297.
El-Juhany, L., 2009. Present status and degradation trends of mangrove forests on the southern Red Sea coast of Saudi Arabia. American-Eurasian Journal of Agricultural and Environmental Science 6, 328-340.
FAO, 2007. The world’s Mangroves 1980-2005. Food and Agriculture Organization.
Fatoyinbo, T.E., Simard, M., 2013. Height and biomass of mangroves in Africa from ICESat/GLAS and SRTM. International Journal of Remote Sensing 34, 668-681.
Friess, D.A., Webb, E.L., 2014. Variability in mangrove change estimates and implications for the assessment of ecosystem service provision. Global ecology and biogeography 23, 715-725.
Giri, C., Ochieng, E., Tieszen, L., Zhu, Z., Singh, A., Loveland, T., Masek, J., Duke, N., 2011. Status and distribution of mangrove forests of the world using earth observation satellite data. Global Ecology and Biogeography 20, 154-159.

Gladstone, W., Tawfiq, N., Nasr, D., Andersen, I., Cheung, C., Drammeh, H., Krupp, F., Lintner, S., 1999. Sustainable use of renewable resources and conservation in the Red Sea and Gulf of Aden: issues, needs and strategic actions. Ocean & coastal management 42, 671-697.
Green, E., Mumby, P., Edwards, A., Clark, C., 1996. A review of remote sensing for the assessment and management of tropical coastal resources. Coastal management 24, 1-40.
Hunink, J., Veenstra, T., van der Hoek, W., Droogers, P., 2010. Q fever transmission to humans and local environmental conditions. FutureWater.
Koch, E.W., Barbier, E.B., Silliman, B.R., Reed, D.J., Perillo, G.M., Hacker, S.D., Granek, E.F., Primavera, J.H., Muthiga, N., Polasky, S., 2009. Non-linearity in ecosystem services: temporal and spatial variability in coastal protection. Frontiers in Ecology and the Environment 7, 29-37.
Kumar, A., Khan, M.A., Muqtadir, A., 2010. Distribution of mangroves along the Red Sea coast of the Arabian Peninsula: Part–1: the northern coast of western Saudi Arabia. Earth Sc. Ind 3, 28-42.
Lulla, K., Duane Nellis, M., Rundquist, B., 2013. The Landsat 8 is ready for geospatial science and technology researchers and practitioners. Geocarto International 28, 191-191.
Mandura, A., 1997. A mangrove stand under sewage pollution stress: Red Sea. Mangroves and Salt marshes 1, 255-262.
Nagelkerken, I., Blaber, S., Bouillon, S., Green, P., Haywood, M., Kirton, L., Meynecke, J.-O., Pawlik, J., Penrose, H., Sasekumar, A., 2008. The habitat function of mangroves for terrestrial and marine fauna: a review. Aquatic Botany 89, 155-185.
PERSGA, 2002. The Red Sea and Gulf of Aden Regional Network of Marine Protected Areas. Regional Master Plan. PERSGA Technical Series, Jeddah.
Pettorelli, N., Vik, J.O., Mysterud, A., Gaillard, J.-M., Tucker, C.J., Stenseth, N.C., 2005. Using the satellite-derived NDVI to assess ecological responses to environmental change. Trends in Ecology & Evolution 20, 503-510.
Polidoro, B.A., Carpenter, K.E., Collins, L., Duke, N.C., Ellison, A.M., Ellison, J.C., Farnsworth, E.J., Fernando, E.S., Kathiresan, K., Koedam, N.E., Livingstone, S.R., Miyagi, T., Moore, G.E., Ngoc Nam, V., Ong, J.E., Primavera, J.H., Salmo, S.G., Sanciangco, J.C., Sukardjo, S., Wang, Y., Yong, J.W., 2010. The loss of species: mangrove extinction risk and geographic areas of global concern. PLoS One 5, e10095.
Price, A., Medley, P., McDowall, R., Dawson-Shepherd, A., Hogarth, P., Ormond, R., 1987. Aspects of mangal ecology along the Red Sea coast of Saudi Arabia. Journal of natural history 21, 449-464.
Raitsos, D.E., Hoteit, I., Prihartato, P.K., Chronis, T., Triantafyllou, G., Abualnaja, Y., 2011. Abrupt warming of the Red Sea. Geophysical Research Letters 38, n/a-n/a.
Sadek, S., Rafael, R., Shakouri, M., Rafomanana, G., Ribeiro, F.L., Clay, J., 2002. Shrimp aquaculture in Africa and the Middle East: the current reality and trends for the future. Report prepared under the World Bank, NACA, WWF and FAO Consortium Program on Shrimp Farming and the Environment. Work in Progress for Public Discussion. Published by the Consortium.
Saifullah, S.M., 1996. Mangrove Ecosystem of Saudi Arabian Red Sea Coast -An Overview Journal of King Abdul Aziz University. 7, 263 -270
Spalding, M., Spalding, M., Kainuma, M., Collins, L., 2010. World atlas of mangroves. Earthscan.
USGS_Landsat_Missions, 2013. Using the USGS Landsat 8 Product. Available online: http://landsat.usgs.gov/Landsat8_Using_Product.php
Valiela, I., Bowen, J.L., York, J.K., 2001. Mangrove forests: One of the world's threatened major tropical environments. Bioscience 51, 807-815.
Vidondo, B., Prairie, Y.T., Blanco, J.M., Duarte, C.M., 1997. Some aspects of the analysis of size spectra in aquatic ecology. Limnology and Oceanography 42, 184-192.

Table legends

Table 1: The error matrix for the presence and absence of mangroves in predicted images (Landsat data) over actual (Google maps).

Table 2: Estimate of mangrove cover growth rate and the % of increase per year, along the Asian and African shores of the Red Sea and the total cover assessed for the three different periods.

Figures legends

Fig 1: a) Mosaic images of mangrove distribution (green areas) in the Red Sea. b) Sections used to estimate coverage. Details in supplementary table 8.

Fig 2: Estimate of mangrove cover (Km^2) along the Asian and African shores of the Red Sea and the total cover assessed for the three different periods.

Fig 3: Pareto Plot describing the size distribution for individual mangrove patches (Km^2) in the Red Sea in 1972 (red), 2000 (green) and 2013 (blue). The solid colored lines show the fitted Pareto regression for each of the time periods (1972, log (%) N>x = -4.03 – 0.69 log Size, R^2 =0.96; 2000, log (%) N>x = -4.07 – 0.70 log Size, R^2 =0.96; 2013, log (%) N>x = -3.95 – 0.68 log Size, R^2 =0.96), the dotted lines indicate the 10% and 1 % size percentiles and the insert shows the median, error bars are the (±C.L) patch size for each period.

Fig 4: Overlapped images showing mangrove gains (green), losses (red), and unchanged areas (yellow)over the time intervals (A) between 1972 and 2000, and (B) between 2000 and 2013.

Fig 5: Examples of Red Sea mangrove vegetation over the study period. (A) dynamics of the largest mangrove stand in the Red Sea (Tabuk, N W. Saudi Arabia). (B) mangrove expansion assoicated to the rehaplitation project in Yanbu (Centeral Red Sea coast of Saudia Arabia). (C) decline of mangrove in a costal lagon at Alith.

Fig6: Map for the drivers of loss and gains in mangrove communities. The symbols from left to right are: (camel: the losses, decay and overgrazing), (factory: represent the pollution), (house for the costal development) and (tree: for the rehablitation/afforistation projects).

ACCEPTED MANUSCRIPT

Table 1:

	Predicted Mangrove (True)	Predicted Non-Mangrove (False)	Total
Actual Mangrove (Positive)	142 (TP)	16 (FP)	158
Actual Non-Mangrove (Negative)	26 (FN)	316 (TN)	342
Total	168	332	500

The overall accuracy was 91.6%

ACCEPTED MANUSCRIPT

Table 2:

		African	Asian	Total
1972-2000 (28 years)	Km^2	8.51	3.97	12.48
	$Km^2\ y^{-1}$	0.30	0.14	0.45
	% y^{-1}	0.42	0.27	0.35
2000-2013 (13 years)	Km^2	1.50	1.12	2.63
	$Km^2\ y^{-1}$	0.12	0.09	0.20
	% y^{-1}	0.15	0.15	0.15
1972-2013 (41 years)	Km^2	10.01	5.09	15.11
	$Km^2\ y^{-1}$	0.24	0.12	0.37
	% y^{-1}	0.33	0.23	0.29

ACCEPTED MANUSCRIPT

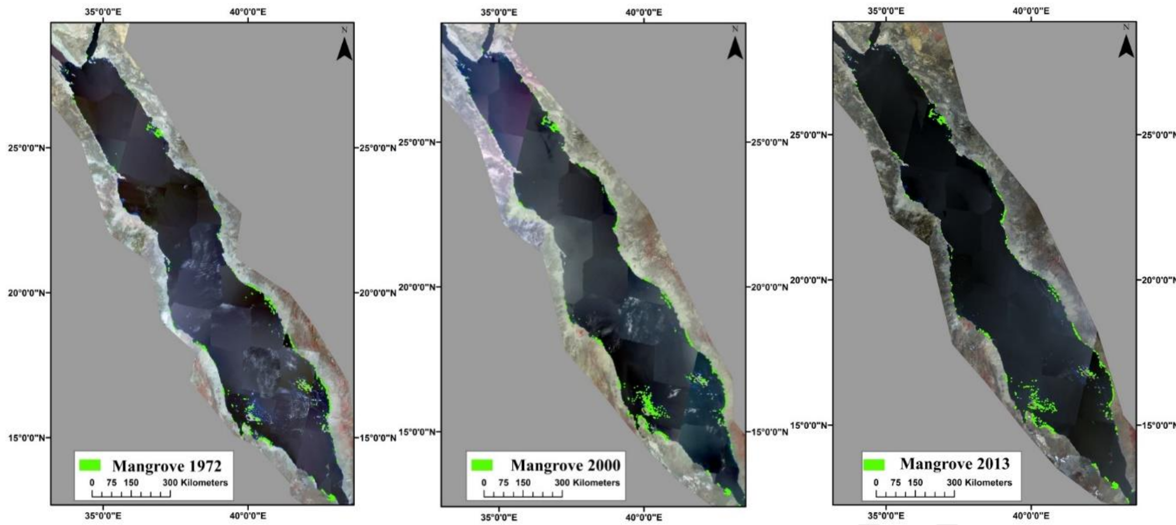

Fig 1a:

ACCEPTED MANUSCRIPT

Fig 1b:

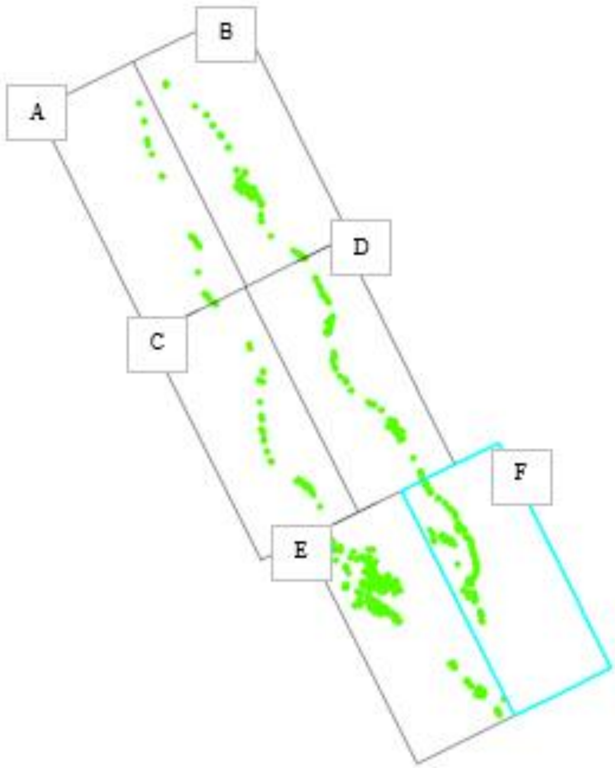

ACCEPTED MANUSCRIPT

ACCEPTED MANUSCRIPT

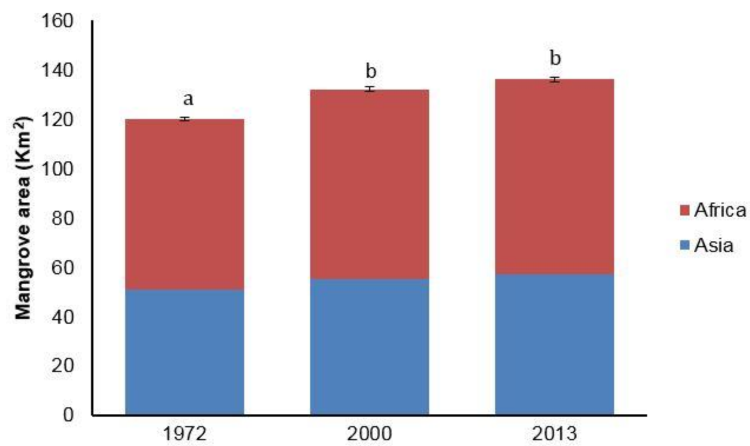

Fig 2:

ACCEPTED MANUSCRIPT

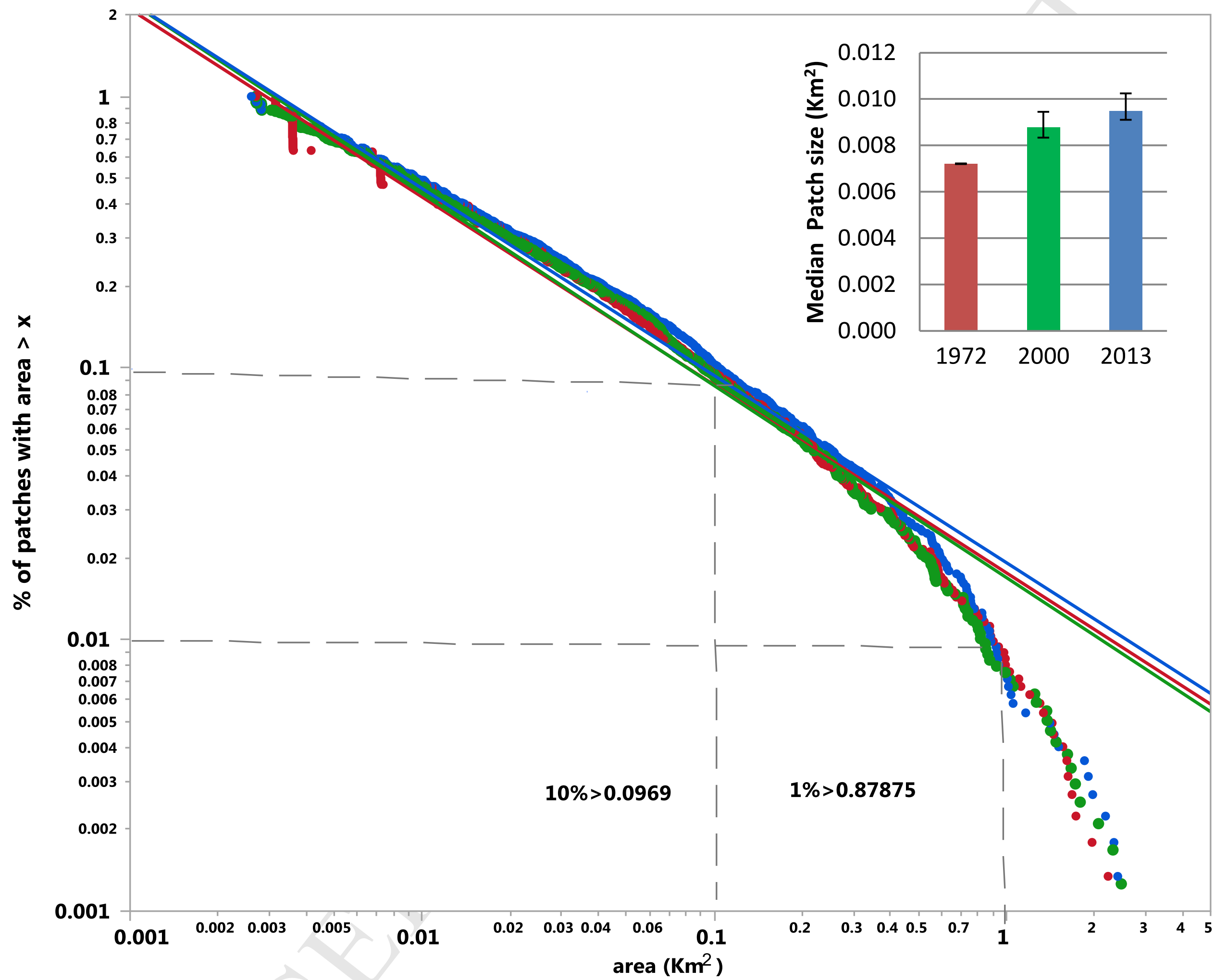

Fig 3:

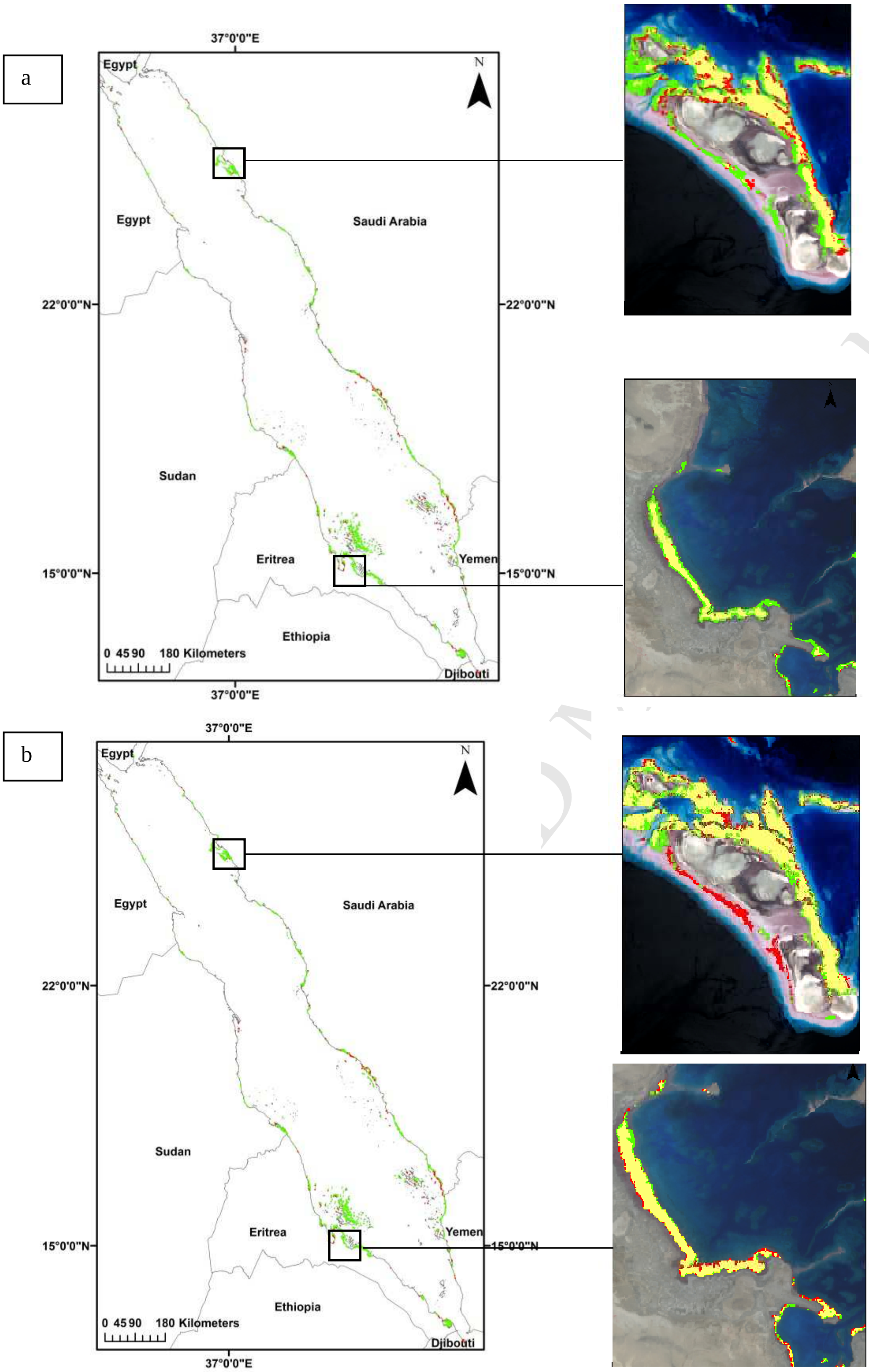
a
37°0'0"E
Egypt
N
Egypt
Saudi Arabia
22°0'0"N
22°0'0"N
Sudan
Eritrea
Yemen
15°0'0"N
15°0'0"N
Ethiopia
0 45 90 180 Kilometers
Djibouti
37°0'0"E
b
37°0'0"E
Egypt
N
Egypt
Saudi Arabia
22°0'0"N
22°0'0"N
Sudan
Eritrea
Yemen
15°0'0"N
15°0'0"N
Ethiopia
0 45 90 180 Kilometers
Djibouti
37°0'0"E

Fig 4:

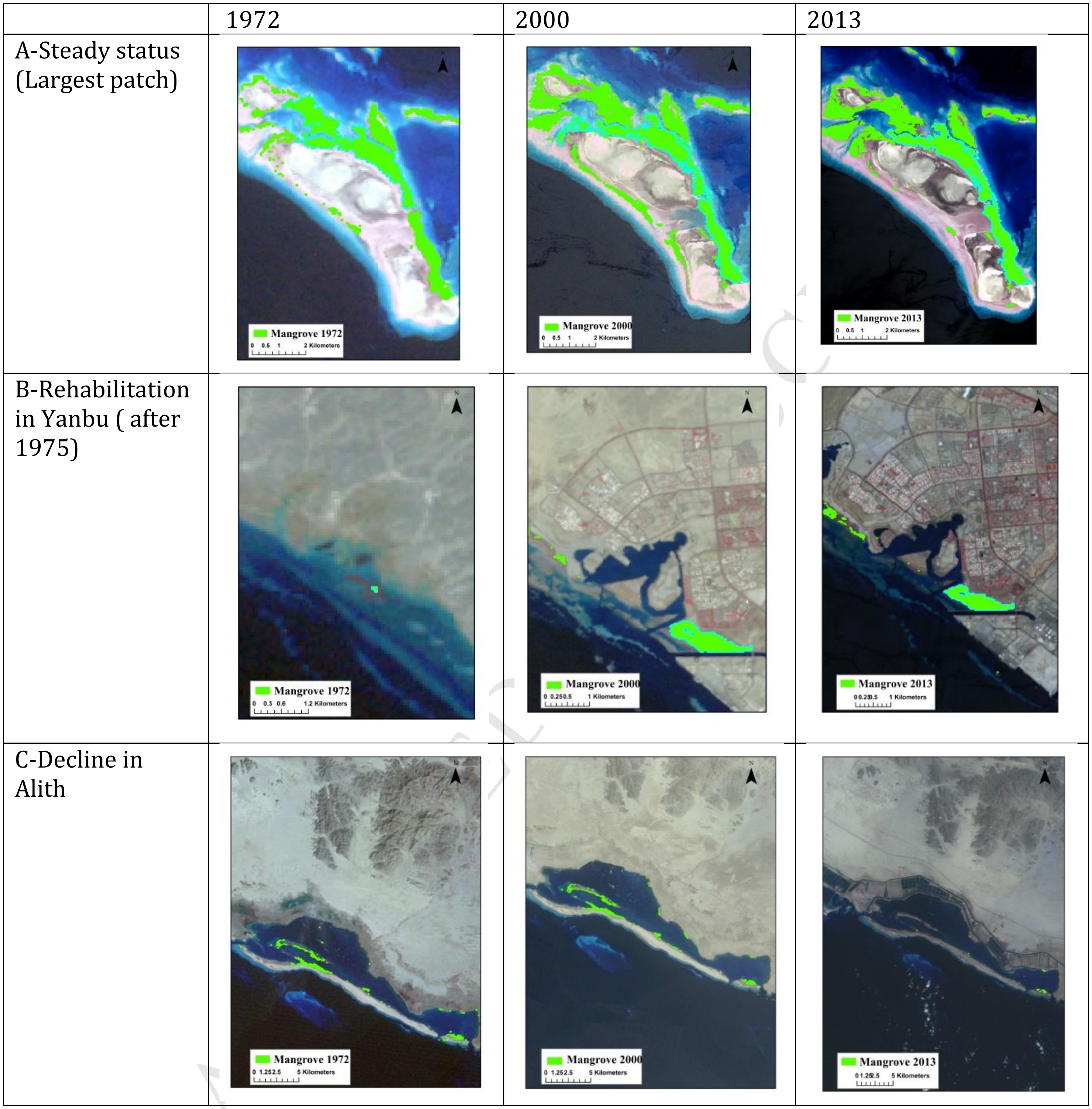
1972
2000
2013
A-Steady status (Largest patch)
B-Rehabilitation in Yanbu (after 1975)
C-Decline in Alith
Mangrove 1972
Mangrove 2000
Mangrove 2013
0 0.5 1 2 Kilometers
0 0.3 0.6 1.2 Kilometers
0 0.25 0.5 1 Kilometers
0 1.25 2.5 5 Kilometers

Fig 5:

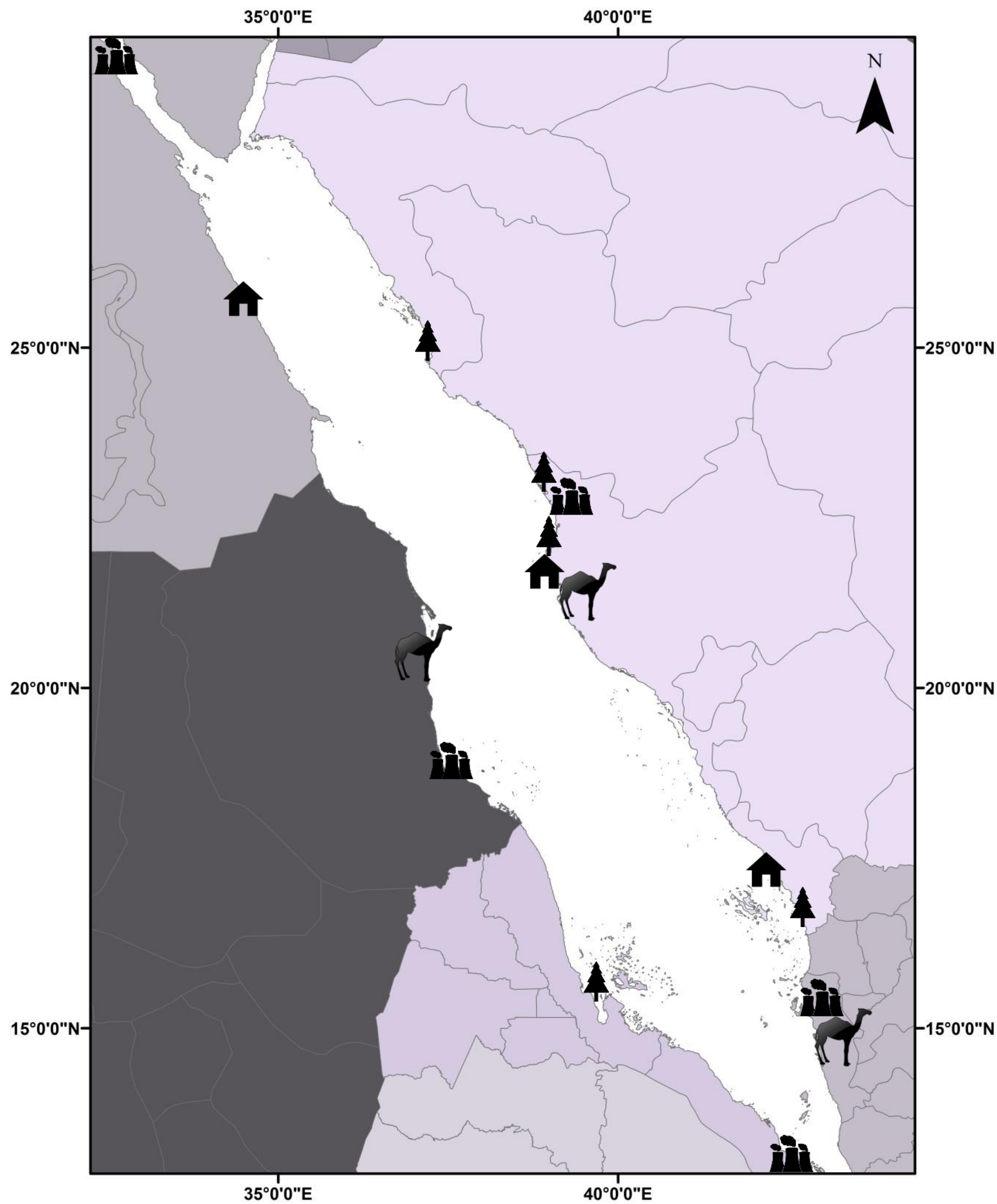

Fig 6.